Organic Electronics 13 (2012) 1185–1191

Contents lists available at SciVerse ScienceDirect

Organic Electronics

journal homepage: www.elsevier.com/locate/orgel

Electrical characteristics of lateral organic bulk heterojunction device structures

Christopher Lombardo [a,b,*], Zi-En Ooi [c], Eric Danielson [a,d], Ananth Dodabalapur [a,c,*]

[a] Microelectronics Research Center, The University of Texas at Austin, Austin, TX 78758, USA
[b] Department of Electrical and Computer Engineering, The University of Texas at Austin, Austin, TX 78712, USA
[c] Institute of Materials Research and Engineering (IMRE), Agency for Science, Technology and Research (A*STAR), 3 Research Link, Singapore 117602, Republic of Singapore
[d] Materials Science and Engineering Program, The University of Texas at Austin, Austin, TX 78712, USA

ARTICLE INFO

Article history:
Received 9 September 2011
Received in revised form 29 February 2012
Accepted 2 March 2012
Available online 21 March 2012

Keywords:
Bulk heterojunction
Organic
Solar cell
Charge transport
Space charge
Photovoltaic

ABSTRACT

Lateral structures have been used to characterize charge transport phenomena in organic bulk heterojunctions. Through the analysis of the current vs. voltage relationships and their light intensity dependence, space charge limited extraction currents and injection currents have been observed and characterized. Additionally, the drift length of charge carriers has been estimated by characterizing devices of varying lengths. These studies show that lateral structures are a promising way to study the basic physics of organic bulk heterojunction materials as they offer degrees of freedom unavailable in sandwich structures and such studies complement what can be learned from conventional sandwich structures.

1. Introduction

Organic photovoltaic cells have been actively studied for over 20 years and as power conversion efficiencies approach 10% [1,2], there is still much to be learned about the transport of charge carriers and recombination mechanisms within these devices. Researchers have employed a multitude of methods to study transport and recombination in bulk heterojunction (BHJ) solar cells, including: photo-generated charge extraction in a linearly increasing voltage (photo-CELIV) [3], ambipolar thin film transistors [4–6], and transient photocurrents [7], to name a few. These reports have focused on measurements of vertical solar cell devices, but these techniques require complex measurement setups that analyze the transient response of solar cells. As solar cells operate in a steady state regime, transient measurements probe transport in an operational regime that is dissimilar to solar cell operation. To enable steady state carrier transport measurements, we have employed a lateral organic photovoltaic (LOPV) cell structure. These structures allow measurements with transport length scales ranging from 10's of nm to more than 100's of μm with uniform charge carrier generation. In this article, we report on the basic characteristics and optoelectronic properties of lateral structures with organic bulk heterojunctions for the first time.

2. Theory

To accurately analyze charge carrier transport in LOPV devices, both the physics of photodetectors and photovoltaic cells must be considered. We first consider the general case of materials with mismatched electron and hole mobilities, which are contacted by non-injecting electrodes. In such materials, space charge limited transport is expected due to the asymmetric mobilities, and as a

* Corresponding authors. Microelectronics Research Center, The University of Texas at Austin, Austin, TX 78758, USA (C. Lombardo).
E-mail addresses: lombardo@mail.utexas.edu (C. Lombardo), ananth.dodabalapur@engr.utexas.edu (A. Dodabalapur).

1566-1199/$ - see front matter © 2012 Elsevier B.V. All rights reserved.
http://dx.doi.org/10.1016/j.orgel.2012.03.003

consequence, there is space charge build-up. The drift length of a charge carrier is the product of its mobility, its lifetime, and the applied electric field ($\lambda = \mu\tau E$). If the drift lengths for both electrons and holes are longer than the device length ($\lambda_e > L \,\&\, \lambda_h > L$), then most carriers will exit the active material with no recombination. If either $\lambda_e < L$ or $\lambda_h < L$ then a space charge region will form and recombination will become prevalent [8]. If carriers can be injected by the contact (as in a photoconductor), then the charge imbalance may be rectified to some extent. This is particularly the case for large voltage biases and low light levels.

A theoretical treatment of the extraction of photogenerated charge carriers with these characteristics was proposed by Goodman and Rose [9] and was initially observed by Mihailetchi et al. in BHJ OPV cells based on BEH_1BMB_3-PPV:PCBM [8]. The difference in carrier mobilities will allow for the formation of a space charge region since one carrier will be able to more quickly exit the device due to its higher mobility leaving behind a space charge region. In this situation, the current vs. voltage characteristics describing bipolar carrier extraction from a space charge limited (SCL) material would be [10]:

$$J_{\text{photo}} = (4\varepsilon\mu)^{1/4}(qG)^{3/4}V^{1/2} \tag{1}$$

where ε is the dielectric constant, μ is the mobility of the slower carrier, and V is the applied voltage bias. Eq. (1) takes into account non-uniform electric fields within the space charge region as described by Ooi et al. [10]. We note that neither treatment considers carrier injection from electrodes.

In LOPV devices considered in this paper, the space charge region will form in only part of the active device; the remainder will be a quasi-neutral region in which electron and hole populations are roughly equal and recombination is extensive. This is especially the case when the spacing between electrodes is large (in excess of 10 μm) [10]. Simulations performed by Ooi et al., indicate that the electric field is not constant in these structures. For this reason, we sometimes employ the "applied voltage per unit length" (V/L). In the case of lateral structures that possess electrodes that permit carrier injection, the previous analysis must be modified, as one of the primary assumptions was that the electrodes are non-injecting. If carriers can be injected into an active bulk heterojunction layer, they will do so once they are provided with sufficient energy to overcome any energetic barriers at the contacts. Carrier injection has been previously described in many material systems, including: poly(phenylenevinylene) and its derivatives [11–13], tetracene [14], cadmium sulfide [15] and many other others. The injection current can be quite large, especially when the mobility mismatch is large. In these cases, photoconductive gain can result in substantial increases in the current flowing in the device and injected currents can compensate for steady-state carrier density imbalances (in what was the space-charge region).

By allowing for carrier injection from the electrodes, the current flowing in a BHJ material with mismatched mobilities should be the sum of the photogenerated current and the injection current. Carriers begin to be injected only after any sufficient energy barriers are overcome, which is represented at an applied bias of V_0. For applied biases of less than V_0, there is negligible injection current. The expected behavior of the total lateral current density is illustrated schematically in Fig. 1 to illustrate the different regimes.

In addition to charge transport studies, LOPV devices can offer a way to probe carrier recombination both within the quasi-neutral region (a.k.a. recombination zone) and the space charge region. In BHJ materials, recombination has been reported to be bimolecular [16,17], but it remains to be seen if the recombination mechanisms are different within the quasi-neutral and space charge regions due to carrier population asymmetries. Studying the recombination rate as a function of light intensity and device length can provide information on the nature of recombination in these materials. Bimolecular recombination processes should prevail when the electron and hole carrier concentrations are roughly balanced, which means the electron and hole mobilities are approximately equal. Although most researchers publish either strictly unimolecular [18] or bimolecular [16,19] recombination mechanisms, it is

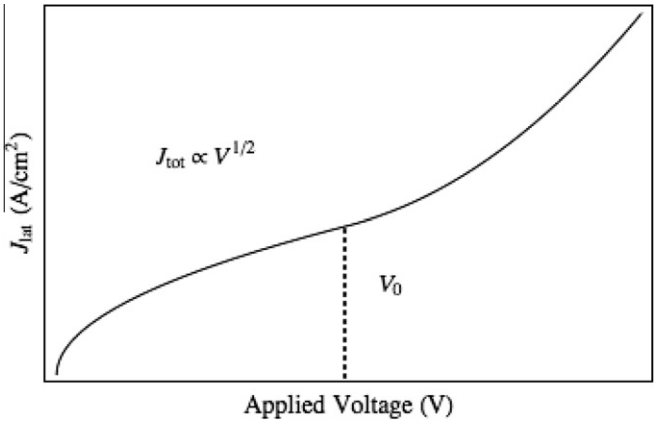

Fig. 1. The total current density (J_{tot}) vs. applied voltage.

likely that an intermediate mechanism or a transition between recombination mechanisms is actually what occurs, as has been reported by Cowan et al. [20].

3. Experimental and measurements

Lateral OPV devices were fabricated starting on a p-type silicon substrate with 2000 Å of thermally grown silicon dioxide. Asymmetric electrodes were defined through two sets of photolithography: one for the aluminum (Al) cathodes and one for the gold (Au) anodes. These metals were chosen to help suppress reverse bias carrier injection within the lateral solar cell [21]. Each of these metals was thermally evaporated with a thickness of 500 Å. The device lengths ranged from 3 μm to 20 μm with a constant $W/L = 1000$. Before deposition of the BHJ layer, the substrate was dipped in a phosphoric acid solution to dissolve any aluminum oxide present on the surface of the Al electrodes. This was followed by a solvent clean to degrease the substrate, which consisted of acetone, methanol, and isopropyl alcohol. The BHJ absorber layer was deposited from a 20 mg/mL solution of P3HT:PCBM (1:1 by weight) dissolved in chloroform that was heated to 50 °C for more than 12 h. The BHJ was spun-cast on the prepared substrates at 1200 rpm for 60 s and this was followed by annealing at 145 °C for 15 min. in a nitrogen atmosphere. The BHJ film was 220 nm thick as measured by profilometry. A schematic illustration of a LOPV cell is shown in Fig. 2.

Electrical measurements were performed in a *Desert Cryogenics* cryogenic probe station under vacuum better than 10^{-3} Torr at 300 K. Electrical measurements were performed using an *Agilent 4155C Semiconductor Parameter Analyzer*. Sample illumination was achieved using an *Oriel model 66912* and *66907* 150 W ozone-free xenon lamp. The optical spectrum was modified using an AM1.5 spectral filter and the light intensity was 100 mW/cm^2. To attenuate the light intensity, a set of neutral density filters was used when necessary. Current vs. voltage measurements were performed on devices with lengths ranging from 3 μm to 20 μm under AM1.5 illumination. Experimental data for the lateral current density vs. applied voltage bias for LOPV cells with device lengths ranging from 3 μm to 20 μm are shown in Fig. 3a and experimental data for the lateral current density vs. applied voltage bias for lateral solar cell with a device length of 5 μm measured with AM1.5 illumination intensities ranging from 6 mW/cm^2 to 100 mW/cm^2 are shown in Fig. 3b. The carrier transport of both electrons and holes has been confirmed through ambipolar thin film transistor measurements, as previously reported [4,6]. The hysteresis between the forward and backward voltage sweeps is the result of carriers falling into deep trap states.

4. Results and discussion

To analyze the current vs. voltage relationships presented in Eq. (1), the functional form of the lateral current density has been determined at multiple voltage values per unit length by finding the slope of the lateral current density vs. voltage curve on a log–log plot. The normalized voltage is defined as the applied bias divided by the device length (V/L). This slope (m) is the resulting functional dependence where $J_{lat} \propto V^m$. For small bias voltages, the voltage exponent decreases with increasing voltage from large values of m to around 0.5. At low applied biases, it is likely that there are energetic barriers for carrier extraction due to contact resistance effects. As the magnitude of applied voltage per unit length increases (in the range of roughly -1.0×10^5 V/cm $\geqslant V/L \geqslant -3.0 \times 10^5$ V/cm), the voltage exponent stabilizes to a value of approximately 0.5. This indicates a regime where SCL extraction currents (Eq. (1)) are present, as predicted by Goodman and Rose [9] and initially observed by Mihailetchi et al. [8]. In this regime, the voltage exponent is not always exactly equal to 0.5 and does increase somewhat with increasing voltage bias. This is likely the result of the electrodes' inability to completely block the injection of charge carriers [22]. The mobility of the slower carrier (hole) evaluated in the space

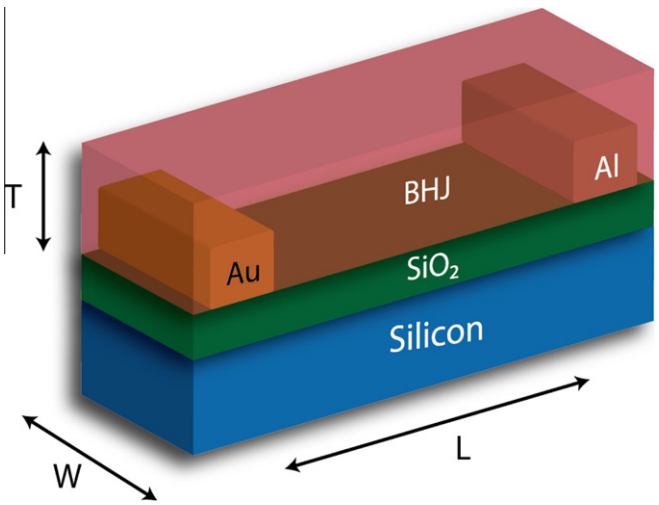

Fig. 2. Schematic illustration of a lateral OPV device.

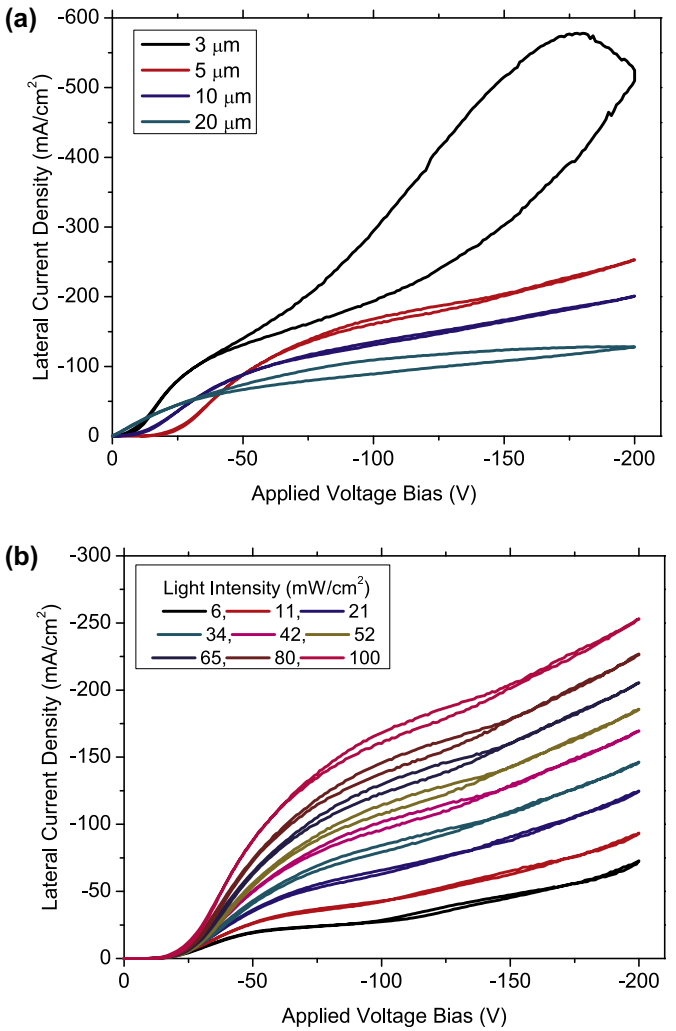

Fig. 3. (a) Lateral current density vs. applied voltage bias for LOPV cells with device lengths ranging from 3 μm to 20 μm under AM1.5 illumination at 100 mW/cm^2. (b) Lateral current density vs. applied voltage bias for a LOPV cell with a device length 5 μm and AM1.5 illumination intensities ranging from 6 mW/cm^2 to 100 mW/cm^2.

charge regime by fitting J–V data to Eq. (1) is listed in Table 1 for various device lengths where the generation rate G is estimated to be 6×10^{21} cm^{-3} s^{-1}using the method reported by Mihailetchi et al. [23] and the dielectric constant, $\varepsilon \approx 3$. The hole mobilities calculated in Table 1 are in the expected range for these devices and are comparable to previous reports where SCL current and photo-CELIV have been used to characterize the mobility within OPV cells made from P3HT:PCBM [16,23–26].

Table 1
Hole mobilities extracted from SCL current measurements using Eq. (1) for various LOPV device lengths. The differing values are a result of different average electric field values.

Device length (μm)	Avg. applied bias (V)	Mobility (cm^2/V s)
3	−65	7.0×10^{-5}
5	−110	8.2×10^{-5}
10	−100	2.7×10^{-5}
20	−105	1.9×10^{-5}

At voltage per unit length magnitudes of greater than -3.0×10^5 V/cm, the voltage exponent continues to increase to a value around 2.0 in some samples. In other samples, this exponent increases well beyond 0.5 but does not cross 1.0. This increase in exponent value is due to substantial current injection into the device. It is also likely that with substantial injection, the space charge approximation (Eq. (1)) may not be valid. Furthermore, when the mobility asymmetry is large and injection occurs, there can be significant photoconductive gain [27]. The voltage exponent (m) is shown as a function of voltage per unit length in Fig. 4a for LOPV devices with device lengths ranging from 3 μm to 20 μm under an AM1.5 illumination intensity of 100 mW/cm^2.

To examine the effect of light intensity on the voltage exponent, the voltage exponent was analyzed as a function

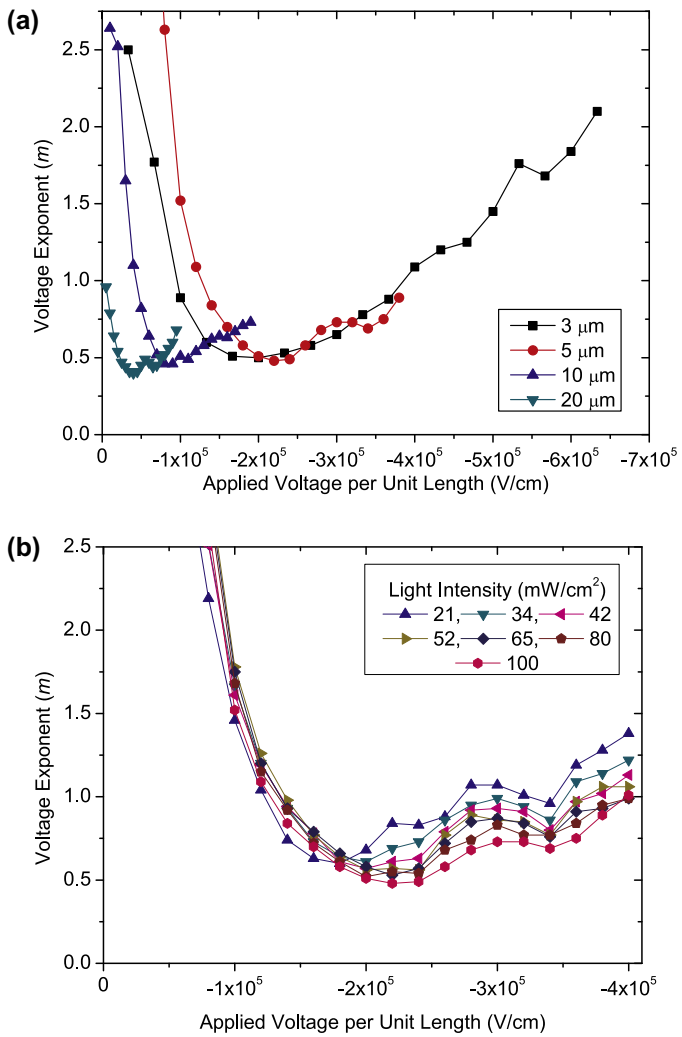

Fig. 4. (a) Voltage exponent (m) vs. applied voltage per unit length for a LOPV cell with device lengths ranging from 3 μm to 20 μm and an AM1.5 illumination intensity of 100 mW/cm^2. (b) Voltage exponent (m) vs. applied voltage per unit length for a LOPV cell with a device length of 5 μm and AM1.5 illumination intensities ranging from 21 mW/cm^2 to 100 mW/cm^2.

of applied voltage per unit length and varying AM1.5 illumination intensities. For increasing illumination intensities, the voltage exponent decreases as a result of the increased photogenerated carrier concentration. Here the number of photogenerated carriers greatly outweighs the number of injected carriers and the current vs. voltage behavior represents this. For lower light intensities, the electrodes inject charge carriers more efficiently due to the reduced number of photogenerated carriers present within the device. The voltage exponent (m) as a function of reverse-bias voltage per unit length for a 5 μm LOPV cell with AM1.5 illumination intensities ranging from 21 mW/cm^2 to 100 mW/cm^2 is shown in Fig. 4b.

The device length dependence of the lateral current density can yield a rough measure of the drift length and mobility-lifetime product. As the device length increases, the current density saturates because the size of the recombination region increases leading to no additional increase in photocurrent [10]. The saturation of the current density as the device length increases yields a drift length which is estimated to be about 5–10 microns which results in a mobility-lifetime product of $\sim 10^{-9}$ cm^2/V. Fig. 5 shows the lateral current density vs. device length for voltage per unit length values ranging from -0.25×10^5 V/cm to -2.0×10^5 V/cm.

In addition to analyzing the functional dependence of the photocurrent density on the applied voltage, the functional dependence of the generation rate can also be analyzed. This is similar to the above procedure where the photocurrent density has been determined at multiple voltage values by finding the slope of the lateral current density vs. light intensity curve on a log–log plot. This slope (n) is the resulting functional dependence where $J_{lat} \propto G^n$. For voltage per unit length magnitudes of less than -1.0×10^5 V/cm, contact resistance is likely contributing to small values of the generation exponent (n). As the magnitude of the voltage per unit length increases (in the range of roughly -1.0×10^5 V/cm $\geqslant V/L \geqslant -3.0$

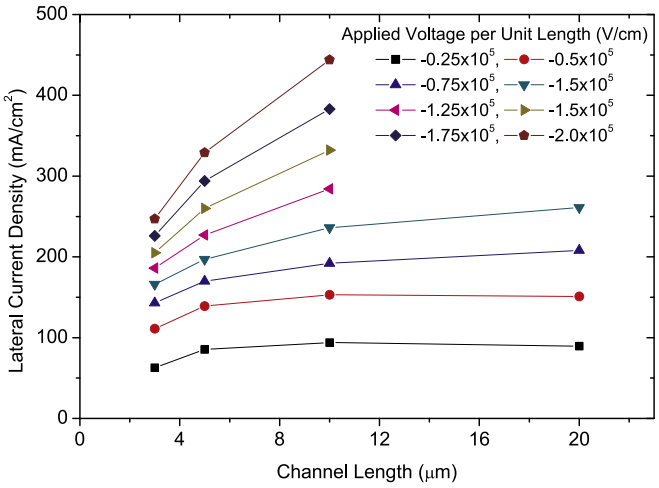

Fig. 5. Lateral current density vs. device length for LOPV cells under AM1.5 illumination at 100 mW/cm^2.

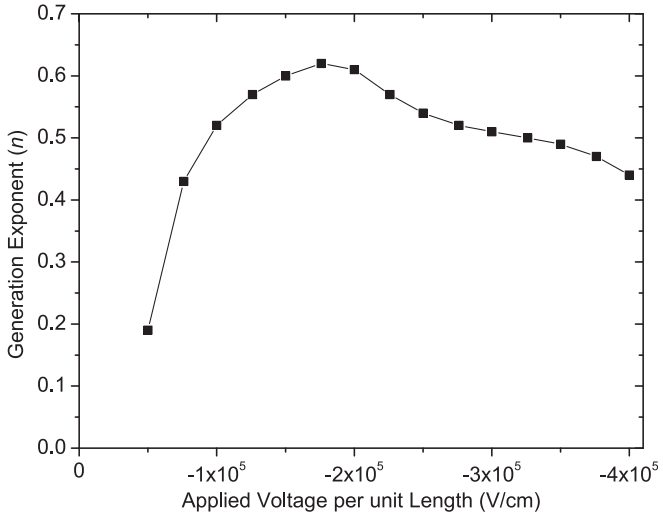

Fig. 6. Generation exponent (n) vs. applied voltage per unit length for a lateral solar cell with a device length of 5 μm.

$\times 10^5$ V/cm), the generation exponent becomes greater than 0.5 but never reaches the predicted value of 0.75. This is likely the result of some carrier injection occurring at these electric field strengths as the nature of the electrodes can change as a result of changing carrier concentration due to varying illumination intensities [28]. At voltage per unit length magnitudes of greater than -3.0×10^5 V/cm, the generation exponent continues to decrease as a result of increasing carrier injection. As the relative number of carriers present in the BHJ layer increases relative to the number of photogenerated carriers, this represents a decrease in the number of charge carriers that are modulated by the incident light. It is also likely the validity of the space charge current density equation (Eq. (1)) becomes questionable as the device deviates from space charge limited transport at high bias. The generation exponent (n) is shown as a function of voltage per unit length in Fig. 6 for a lateral solar device with a device length of 5 μm.

5. Conclusion

A combination of photodectector and organic photovoltaic device theory has been used to characterize the operation of lateral bulk heterojunction device structures with imbalanced carrier mobilities. Such measurements are shown to yield useful information on the charge transport phenomena present in BHJ OPV materials. Both SCL photocurrent extraction and current injection have been observed in different device operation regimes. Data comparison to simulations of lateral OPV devices has agreed with the proposed theory that includes two transport zones. Devices that are roughly 5 μm or less are dominated by a space charge zone in which most of the photogenerated carriers are transported out of the device. Longer devices, which are greater than 5 μm, are strongly influenced by a recombination zone where most of the photogenerated carriers recombine before exiting the device. Further studies

on these lateral devices are expected to yield information about the drift lengths of each carrier type as well as other transport and recombination parameters that are not easily measurable using vertical structures.

Acknowledgements

The authors would like to thank Brian Cobb for useful discussions as well as the facilities staff at the Microelectronics Research Center at The University of Texas at Austin. In addition, the authors acknowledge the ONR under STTR Project No. N00014-10-M-0317 and CONTACT for financial support of this project. Additional funding was provided by A*STAR under the visiting investigator program (VIP).

References

[1] M.A. Green, K. Emery, Y. Hishikawa, W. Warta, E.D. Dunlop, Solar cell efficiency tables (Version 38), Progress in Photovoltaics: Research and Applications 19 (2011) 565–572.
[2] C.J. Brabec, S. Gowrisanker, J.J.M. Halls, D. Laird, S. Jia, S.P. Williams, Polymer–fullerene bulk-heterojunction solar cells, Advanced Materials 22 (2010) 3839–3856.
[3] R. Österbacka, A. Pivrikas, G. Juska, K. Genevicius, K. Arlauskas, H. Stubb, Mobility and density relaxation of photogenerated charge carriers in organic materials, Current Applied Physics 4 (2004) 534–538.
[4] C. Lombardo, A. Dodabalapur, Nongeminate carrier recombination rates in organic solar cells, Applied Physics Letters 97 (2010) 233302–233303.
[5] H. Bronstein, Z. Chen, R.S. Ashraf, W. Zhang, J. Du, J.R. Durrant, P. Shakya Tuladhar, K. Song, S.E. Watkins, Y. Geerts, M.M. Wienk, R.A.J. Janssen, T. Anthopoulos, H. Sirringhaus, M. Heeney, I. McCulloch, Thieno[3,2-b]thiophene, àíDiketopyrrolopyrrole-containing polymers for high-performance organic field-effect transistors and organic photovoltaic devices, Journal of the American Chemical Society 133 (2011) 3272–3275.
[6] C. Lombardo, E. Danielson, Z.E. Ooi, A. Dodabalapuar, Lateral mobility measurements in organic bulk heterojunctions: comparison of field-effect and space charge mobilities, Journal of Photonics for Energy 2(2) (2012).
[7] R.A. Street, S. Cowan, A.J. Heeger, Experimental test for geminate recombination applied to organic solar cells, Physical Review B 82 (2010) 121301.
[8] V.D. Mihailetchi, J. Wildeman, P.W.M. Blom, Space-charge limited photocurrent, Physical Review Letters 94 (2005) 126602.
[9] A.M. Goodman, A. Rose, Double extraction of uniformly generated electron–hole pairs from insulators with noninjecting contacts, Journal of Applied Physics 42 (1971) 2823–2830.
[10] Z.-E. Ooi, K.L. Chan, C.J. Lombardo, A. Dodabalapur, Photocurrents in lateral-geometry and thick-layer organic photovoltaic devices, Organic Electronics, submitted for publication.
[11] A.J. Campbell, D.D.C. Bradley, D.G. Lidzey, Space-charge limited conduction with traps in poly(phenylene vinylene) light emitting diodes, Journal of Applied Physics 82 (1997) 6326–6342.
[12] S.C. Jain, W. Geens, A. Mehra, V. Kumar, T. Aernouts, J. Poortmans, R. Mertens, M. Willander, Injection- and space charge limited-currents in doped conducting organic materials, Journal of Applied Physics 89 (2001) 3804–3810.
[13] C. Tanase, E.J. Meijer, P.W.M. Blom, D.M. de Leeuw, Unification of the hole transport in polymeric field-effect transistors and light-emitting diodes, Physical Review Letters 91 (2003) 216601.
[14] A.K. Ghosh, T. Feng, Rectification, space-charge-limited current, photovoltaic and photoconductive properties of Al/tetracene/Au sandwich cell, Journal of Applied Physics 44 (1973) 2781–2788.
[15] R.W. Smith, A. Rose, Space-charge-limited currents in single crystals of cadmium sulfide, Physical Review 97 (1955) 1531.
[16] A. Pivrikas, N.S. Sariciftci, G. Juscaronka, R. Österbacka, A review of charge transport and recombination in polymer/fullerene organic solar cells, Progress in Photovoltaics: Research and Applications 15 (2007) 677–696.
[17] C.G. Shuttle, R. Hamilton, B.C. O'Regan, J. Nelson, J.R. Durrant, Charge-density-based analysis of the current–voltage response of polythiophene/fullerene photovoltaic devices, Proceedings of the National Academy of Sciences 107 (2010) 16448–16452.
[18] R.A. Street, M. Schoendorf, A. Roy, J.H. Lee, Interface state recombination in organic solar cells, Physical Review B 81 (2010) 205307.
[19] P.W.M. Blom, V.D. Mihailetchi, L.J.A. Koster, D.E. Markov, Device physics of polymer:fullerene bulk heterojunction solar cells, Advanced Materials 19 (2007) 1551–1566.
[20] S.R. Cowan, A. Roy, A.J. Heeger, Recombination in polymer-fullerene bulk heterojunction solar cells, Physical Review B 82 (2010) 245207.
[21] S. Cho, J. Yuen, J.Y. Kim, K. Lee, A.J. Heeger, Photovoltaic effects on the organic ambipolar field-effect transistors, Applied Physics Letters 90 (2007) 063511–063513.
[22] V.D. Mihailetchi, P.W.M. Blom, J.C. Hummelen, M.T. Rispens, Cathode dependence of the open-circuit voltage of polymer:fullerene bulk heterojunction solar cells, Journal of Applied Physics 94 (2003) 6849–6854.
[23] V.D. Mihailetchi, H.X. Xie, B. de Boer, L.J.A. Koster, P.W.M. Blom, Charge transport and photocurrent generation in poly(3-hexylthiophene):methanofullerene bulk-heterojunction solar cells, Advanced Functional Materials 16 (2006) 699–708.
[24] V. Chellappan, Imbalanced charge mobility in oxygen treated polythiophene/fullerene based bulk heterojunction solar cells, Applied Physics Letters 95 (2009) 263305.
[25] D. Chirvase, Z. Chiguvare, M. Knipper, J. Parisi, V. Dyakonov, J.C. Hummelen, Electrical and optical design and characterisation of regioregular poly(3-hexylthiophene-2,5diyl)/fullerene-based heterojunction polymer solar cells, Synthetic Metals 138 (2003) 299–304.
[26] L.J.A. Koster, V.D. Mihailetchi, P.W.M. Blom, Bimolecular recombination in polymer/fullerene bulk heterojunction solar cells, Applied Physics Letters 88 (2006) 052103–052104.
[27] S.M. Sze, K.K. Ng, Physics of Semiconductor Devices, third ed., John Wiley & Sons, Hoboken, 2007.
[28] Y. Shen, A.R. Hosseini, M.H. Wong, G.G. Malliaras, How to make ohmic contacts to organic semiconductors, ChemPhysChem 5 (2004) 16–25.